Lin *et al. Virology Journal* (2024) 21:273
https://doi.org/10.1186/s12985-024-02549-x

Virology Journal

BRIEF REPORT Open Access

Preferential cleavage of the coronavirus defective viral genome by cellular endoribonuclease with characteristics of RNase L

Ching-Hung Lin[1], Hsuan-Yung Lin[2], Chun-Chun Yang[2], Hsuan-Wei Hsu[2], Feng-Cheng Hsieh[2], Cheng-Yao Yang[2] and Hung-Yi Wu[2*]

Abstract

In testing whether coronavirus defective viral genome 12.7 (DVG12.7) with transcription regulating sequence (TRS) can synthesize subgenomic mRNA (sgmRNA) in coronavirus-infected cells, it was unexpectedly found by Northern blot assay that not only sgmRNA (designated sgmDVG 12.7) but also an RNA fragment with a size less than sgmDVG 12.7 was identified. A subsequent study demonstrated that the identified RNA fragment (designated clvDVG) was a cleaved RNA product originating from DVG12.7, and the cleaved sites were located in the loop region of stem–loop structure and after UU and UA dinucleotides. clvDVG was also identified in mock-infected HRT-18 cells transfected with DVG12.7 transcript, indicating that cellular endoribonuclease is responsible for the cleavage. In addition, the sequence and structure surrounding the cleavage sites can affect the cleavage efficiency of DVG12.7. The cleavage features are therefore consistent with the general criteria for RNA cleavage by cellular RNase L. Furthermore, both the cleavage of rRNA and the synthesis of clvDVG were also identified in A549 cells. Because (i) the cleavage sites occurred predominantly after single-stranded UA and UU dinucleotides, (ii) the sequence and structure surrounding the cleavage sites affected the cleavage efficiency, (iii) the cleavage of rRNA is an index of the activation of RNase L, and (iv) the cleavage of both rRNA and DVG12.7 was identified in A549 cells, the results together indicated that the preferential cleavage of DVG12.7 is correlated with cellular endoribonuclease with the characteristics of RNase L and such cleavage features have not been previously characterized in coronaviruses.

Keywords Coronavirus, Defective viral genome, RNA cleavage, Endoribonuclease, RNase L

*Correspondence:
Hung-Yi Wu
hwu2@dragon.nchu.edu.tw
[1]Department of Veterinary Medicine, National Pingtung University of Science and Technology, Neipu 91201, Pingtung, Taiwan
[2]Graduate Institute of Veterinary Pathobiology, College of Veterinary Medicine, National Chung Hsing University, Taichung 40227, Taiwan

Background

Coronaviruses in the order *Nidovirales* are single-stranded, positive-sense RNA viruses with genome sizes of 26–32 kb [1, 2]. During coronavirus transcription, a series of subgenomic mRNAs (sgmRNAs) are synthesized from transcription-regulating sequences (TRSs), which are located upstream of each structural and accessory protein gene [3], using the genome as a template and directed by the TRS through a similarity-assisted template-switching recombination mechanism [4–6]. In addition to sgmRNAs, coronaviruses can also synthesize defective viral genomes (DVGs) [7, 8]. The DVG in coronaviruses is previously named defective interfering (DI) RNA [7] and is a truncated version of the virus genome. Coronavirus DVG has been suggested to play a critical role in modulating host IFN responses and symptom development [9]. Previously identified DVGs in coronaviruses contain *cis*-acting elements necessary for gene expression in their 5' and 3' termini, and they have been intensively employed as surrogates of the ~30 kb full-length genome for studies on coronavirus gene expression [5, 6, 10–12]. In addition, sgmRNA can be produced from coronavirus DVGs with TRSs; thus, TRS-containing DVGs in coronaviruses, including bovine coronavirus (BCoV), have been intensively employed to study the mechanism of coronavirus sgmRNA synthesis [13, 14].

The expression of type I interferon can induce interferon-stimulated genes (ISGs), including 2'-5'-oligoadenylate synthetase (OAS) [15, 16]. OAS senses double-stranded RNA (dsRNA) and then uses ATP to synthesize 2',5'-linked oligoadenylates (2–5 A), which causes inactive RNase L monomers to form activated dimers. Activated RNase L is able to cleave viral and host RNA, leading to the inhibition of virus replication and subsequent gene expression [17, 18]. The endoribonuclease RNase L contains a kinase-like domain and an endonuclease domain [19], and is a well-studied endoribonuclease associated with antiviral defense induced by innate immunity [16, 20, 21]. The endoribonuclease RNase L targets single-stranded RNA, synthesizing 5'- hydroxyl and 2', 3'-cyclic phosphate termini at the cleavage site [22]. RNase L cleaves viral and host RNA predominantly after single-stranded UA and UU dinucleotides, and the cleavage of host rRNA is an index of the activation of RNase L [16, 18, 23, 24]. The context where the dinucleotides UA and UU reside may also affect the efficiency of cleavage. In hepatitis C virus, the genome structures surrounding UA or UU dinucleotides can affect the cleavage efficiency of RNase L [23, 25]. The sequence features of viral RNA specific for cleavage by RNase L have not been previously probed in coronaviruses.

During the investigation of whether the coronavirus DVG12.7 with TRS can synthesize sgmRNA [14], an RNA fragment shorter than DVG-derived sgmRNA at 1 h posttransfection was observed by Northern blot assay. According to our regular procedure with 600 ng of DVG12.7 transcript for transfection, sgmRNA derived from DVG12.7 is not likely to be detected by Northern blot assay in one hour. Therefore, in the current study, we sought a possible mechanism for the synthesis of the shorter RNA fragments. Subsequent experiments suggested that the shorter RNA fragment was a cleaved fragment of DVG12.7. Characterizing the features of the cleaved site and cleaved pattern revealed that the cleavage may be correlated with the characteristics of cellular endoribonuclease RNase L.

Methods

Virus and cells The BCoV strain of Mebus (GenBank accession no. U00735) was grown in human rectum tumor (HRT)-18 cells [26] and was obtained from David A. Brian (University of Tennessee, TN). BCoV was plaque-purified and the virus titer was 4.5×10^8 PFU/mL. HRT-18 cells and adenocarcinomic human alveolar basal epithelial (A549) cells were grown in Dulbecco's modified Eagle's medium (DMEM) supplemented with 10% fetal bovine serum (HyClone, UT, USA) at 37 °C with 5% CO_2.

Identification of the RNA fragments derived from DVG12.7 by Northern blot assay To construct the DVG12.7 mutants, an overlap PCR mutagenesis procedure was performed as previously described [14, 27]. To examine the synthesis of sgmDVG12.7 from DVG12.7, HRT-18 cells were infected with BCoV at a multiplicity of 10 and transfected with 600 ng of transcript at 1 h postinfection (hpi). Total cellular RNA was collected at 1 and 24 h posttransfection (hpt). To examine the cleavage efficiency of DVG12.7 and its mutants for the synthesis of clvDVG, HRT-18 cells were transfected with 600 ng of transcript, and total cellular RNA was collected. The aforementioned total cellular RNA was subjected to Northern blot assay. The Northern blot assay was performed as previously described [28]. In brief, 10 μg per lane was used for electrophoresis in a formaldehyde-agarose gel. The resulting RNA was then transferred to a Nylon Hybond N+membrane (Cytiva Life Sciences, Marlborough, MA, USA) by vacuum blotting for 3 h followed by UV crosslinking (XL-1000, SpectrolinkerTM), prehybridization at 45 °C for 6 h and hybridization (NorthernMax™ Kit, Thermo Fisher Scientific, Waltham, USA) at 45 °C for 16 h. The membranes were then probed with oligonucleotide 5'GPD4(+) labeled with ^{32}P. The membrane was exposed to Kodak XAR-5 film in the presence of an intensifying screen.

Identification of cleaved sites of DVG12.7 by RACE and PCR To examine the cleaved sites of DVG12.7, linearized pDVG12.7 was transcribed in vitro with T7 RNA

polymerase (Promega), and the synthesized DVG12.7 transcripts were transfected into BCoV-infected HRT-18 cells. At 1 hpt, total cellular RNA was collected and extracted with TRIzol (Thermo Fisher Scientific, Waltham, USA). The oligonucleotide 5'GPD4(+):5'CGA TTCGGGTTGGCCATTCTTGAGAGAGGC3' was used for reverse transcription (RT) with SuperScript III reverse transcriptase. The resulting cDNA was used for rapid amplification of cDNA ends (RACE) to identify the 5' cleaved sites according to the manufacturer's instructions. PCR was performed with RACEG (–): 5'GGCCACGC-GTTCCTACTAGTACCCCCCCCCCC3' and 5'GD (+): 5'GAGACTAGGCATCCGCCAAGGCATATTTG3' for 34 cycles of 30 s at 94 °C, 30 s at 55 °C and 90 s at 72 °C. The amplified fragments were cloned with the TOPO™ XL-2 Complete PCR Cloning Kit (Thermo Fisher Scientific, Waltham, USA), followed by sequencing analysis.

Detection of the cleavage of DVG12.7 and rRNA in HRT-18 and A549 cells Freshly confluent HRT-18 and A549 cells were transfected with 600 ng of DVG12.7 transcript. After 0.1, 1.5 and 3 h of transfection, total cellular RNA was collected, and 10 μg per lane was used for electrophoresis in a formaldehyde-agarose gel to detect the cleavage of rRNA or for Northern blot assay to detect the synthesis of clvDVG.

Detection of OAS mRNA To detect OAS mRNA, 5 μg of total cellular RNA prepared from the cleavage of DVG12.7 and rRNA in HRT-18 and A549 cells was subjected to reverse transcription with SuperScript III Reverse Transcriptase (Thermo Fisher Scientific, Waltham, USA) and random hexamers. PCR was performed with AccuPrime DNA polymerases (Invitrogen, California, USA) and the primers OAS3-2381(-): 5'-CCAACCGCCAGTTCCTG GCCCAGG-3' and OAS3-2521(+): 5'-GAGGTCGGCA TCTGAGCGGCCTCG-3' for 34 cycles of 30 s at 94 °C, 30 s at 55 °C and 30 s at 72 °C. For qPCR, SYBR® green amplification mix (Roche Applied Science, Mannheim, Germany) was used according to the manufacturer's protocol. Dilutions of plasmids containing the same gene as the detected OAS3 mRNA were run in parallel with the quantitated cDNA for use in standard curves (dilutions ranging from 10^8 to 10 copies of each plasmid).

Results

Synthesis of an RNA fragment from the cleavage of defective viral genome 12.7 In an attempt to examine whether the bovine coronavirus (BCoV) defective viral genome (DVG) 12.7 with transcription regulating sequence (TRS) can synthesize subgenomic DVG 12.7 (sgmDVG 12.7) derived from TRS (Fig. 1A), it was unexpectedly found by Northern blot assay that, in addition to the predicted sgmDVG 12.7, an RNA fragment shorter than sgmDVG 12.7 was identified in BCoV-infected HRT-18 cells (indicated with red arrow in Fig. 1B). Because (i) the primer probe for the Northern blot assay was located in the reporter gene (Fig. 1A) and (ii) the size of the RNA fragment was less than that of sgmDVG 12.7 (Fig. 1B), it was therefore hypothesized that the RNA fragment was derived from DVG12.7.

To determine the possible site from which the RNA fragment was derived, RNA extracted from DVG12.7-transfected BCoV-infected HRT-18 cells at 1 h post-transfection (hpt) was subjected to rapid amplification of cDNA ends (RACE) and PCR followed by sequencing. The sequencing results suggested that the RNA fragment identified in Fig. 1B was a cleaved RNA product originating from DVG12.7 (Fig. 1C). The cleaved sites were located at nucleotide positions 1783 and 1784 in DVG12.7, (Fig. 1C). Furthermore, the cleaved site is located downstream of the TRS, in the loop region of stem–loop II and after UU and UA dinucleotides (Fig. 1D). Thus, the shorter RNA fragment was a cleaved RNA product derived from DVG12.7 and was designated cleaved DVG (clvDVG) (Fig. 1E).

The cleavage of DVG12.7 is caused by cellular endoribonuclease To determine the cellular or viral factor(s) leading to cleavage, uninfected- or BCoV-infected HRT-18 cells were transfected with DVG12.7, and total cellular RNA was collected at different time points posttransfection. As shown in Fig. 2, clvDVG was observed at 0.5 to 6 hpt in mock-infected HRT cells (Fig. 2, left panel). In BCoV-infected HRT-18 cells, clvDVG was also observed at 0.5 to 6 hpt but gradually disappeared after 6 hpt (Fig. 2, right panel). Instead, sgmDVG12.7 began to be synthesized at 9 h of transfection (Fig. 2, right panel). The cleaved DVG12.7 fragment slvDVG was identified in both uninfected and infected HRT18 cells, indicating that cellular endoribonuclease is responsible for the cleavage. Note that the ratio of cleaved vs. uncleaved DVG12.7 was constant (10–15%) and did not increase with time (Fig. 2, lower panel). In addition, it has been suggested that coronaviral RNA synthesis can occur in a modified compartment at the membrane of endoplasmic reticulum [29]. This modified compartment has the advantage of protecting viral RNA from antiviral defense mechanisms, such as RNA degradation by cellular RNases [29, 30]. Thus, although the amounts of DVG12.7 are abundant at 9 and 24 hpt in infected HRT-18 cells, cleavage does not occur, and clvDVG is not synthesized, leading to almost undetectable levels of clvDVG at 9 and 24 hpt in infected HRT-18 cells.

Characterization of the cleaved features of clvDVG It has been experimentally determined that there are two stem–loops in the region where the TRS is located

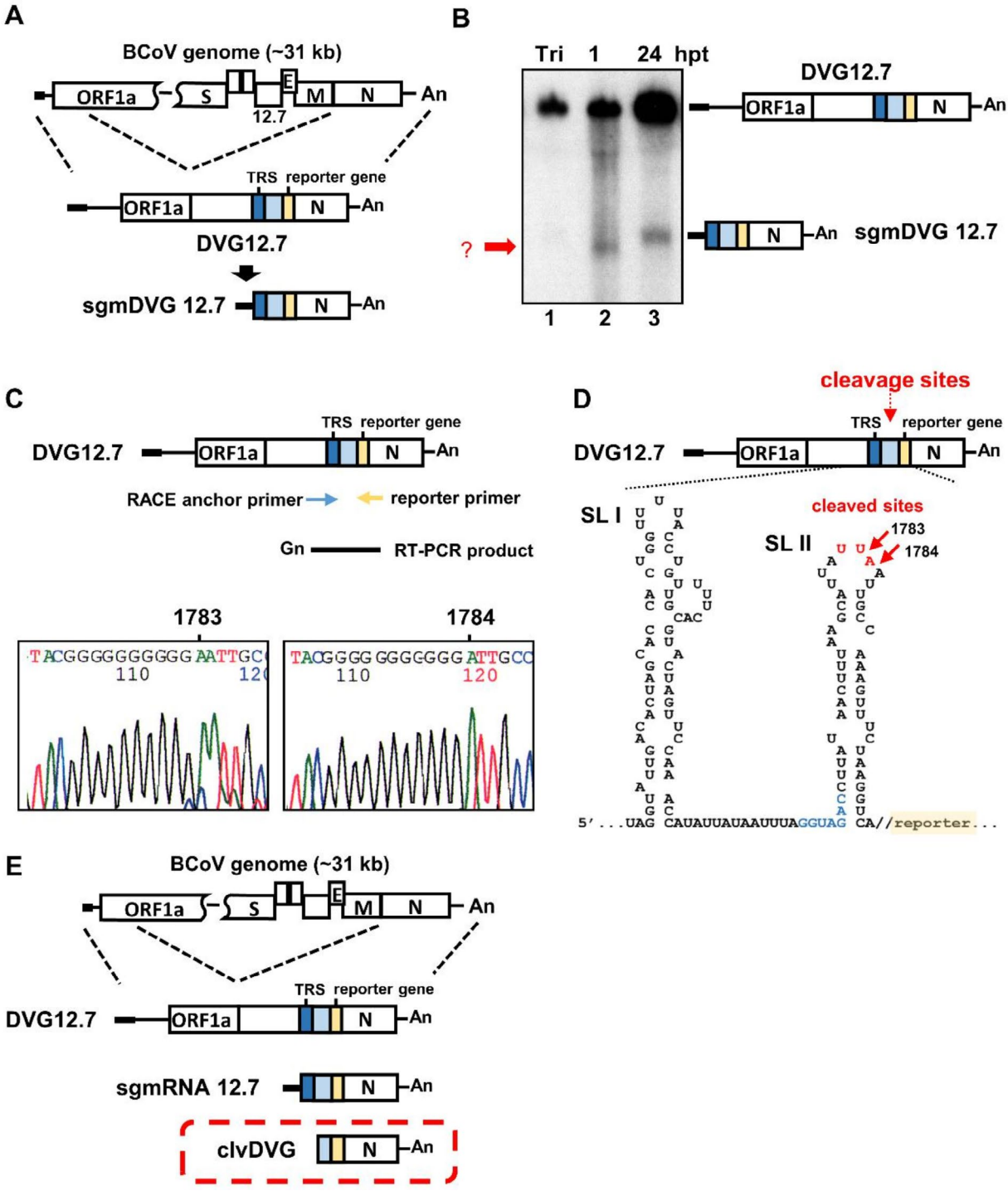

Fig. 1 Identification of the cleaved site of DVG12.7 for synthesis of clvDGV. **(A)** Genome structures of the BCoV genome, DVG12.7 and putative sgmDVG 12.7 derived from DVG12.7. The TRS in DVG12.7 is derived from sgmRNA 12.7 TRS. **(B)** By Northern blot assay, in addition to the DVG12.7 and sgmDVG 12.7, an RNA fragment shorter than sgmDVG 12.7 was observed (indicated with red arrow). Note that Tri in Lane 1 indicates the in vitro transcribed DVG12.7 transcript, and the DVG12.7 transcript (10 ng) was directly subjected to Northern blotting. The DVG12.7 transcript is shown to ensure that the cleaved product clvDVG is not derived from the DVG12.7 transcript. **(C)** Strategy to identify the cleavage site of the DVG12.7 for the synthesis of RNA fragment shorter than sgmDVG 12.7 shown in (B). cDNA was synthesized by the RACE method with a primer annealing to the reporter gene, and PCR was performed followed by cloning and sequencing. Sequencing analysis showing that the cleaved sites were located at nucleotide positions 1783 and 1784 in DVG12.7. **(D)** There are two stem–loops (SL I and II) in the region of TRS, and the cleavage sites were located at the loop region of SL II and after UU and UA dinucleotides. **(E)** The structure of RNA fragment clvDVG (dotted line frame) derived from DVG12.7. DVG, defective viral genome; TRS, transcription regulating sequence; SL, stem–loop; sgm, subgenomic mRNA; Tri, DVG12.7 transcript

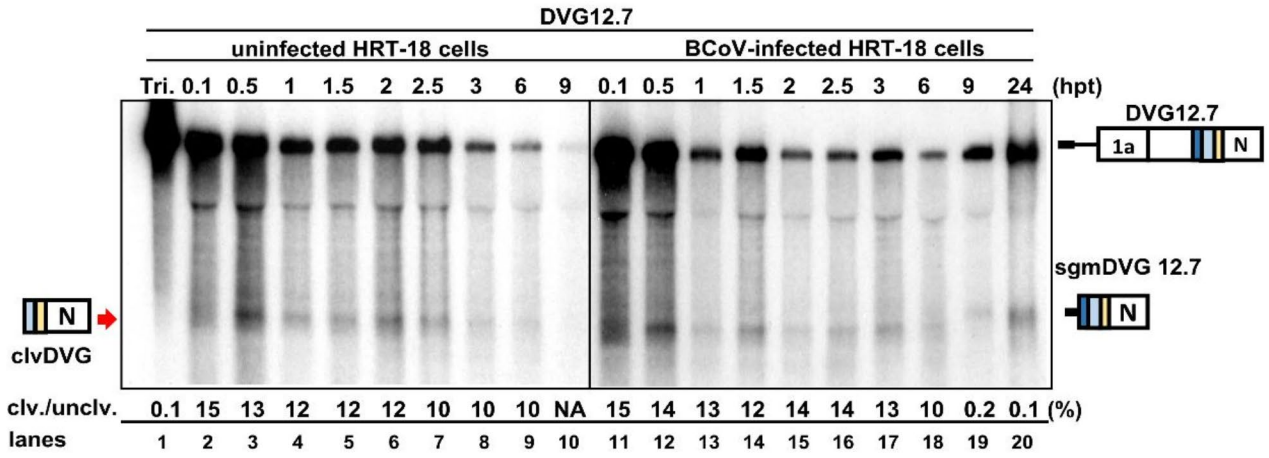

Fig. 2 The cleavage of DVG12.7 is caused by cellular endoribonuclease. Cleaved DVG12.7 (clvDVG) was identified in both uninfected (left panel, Lanes 3–9) and infected (right panel, Lanes 12–18) HRT-18 cells at different time points post-transfection by Northern blot assay. sgmDVG12.7 started to be synthesized at 9 h of transfection (Lanes 19–20, right panel). Lower panel: The ratio of cleaved (clv.) to uncleaved (unclv.) DVG12.7 in uninfected (left panel) and infected (right panel) HRT-18 cells based on the Northern blotting results. Tri., DVG12.7 transcript

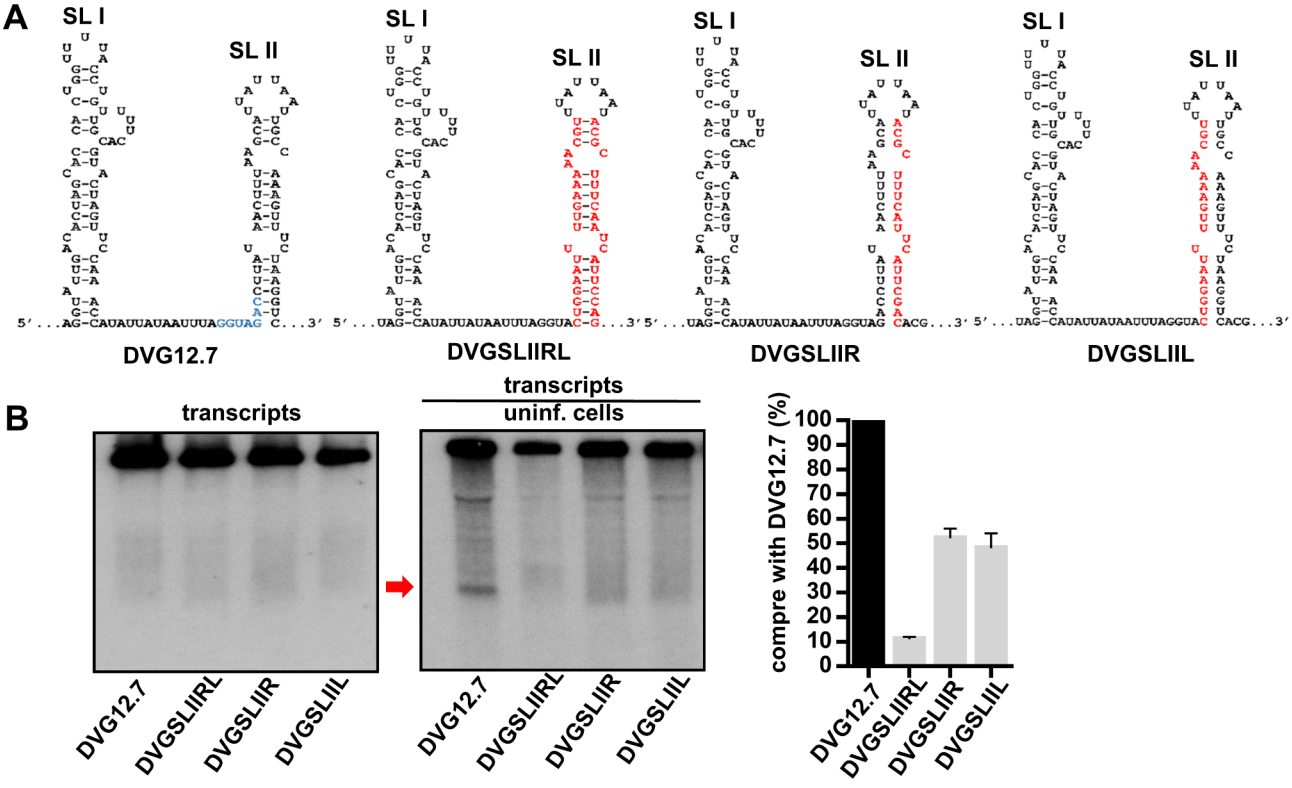

Fig. 3 The effect of genome structures and sequences surrounding the cleaved sites on the cleavage efficiency of DVG12.7. **(A)** Constructs of compensatory mutants of DVG12.7: DVGSLIIRL, in which sequences in both stems were exchanged, maintaining the SL-II structure; DVGSLIIL, in which the sequences in the left stem were replaced by those from the right stem, altering the SL-II structure; and DVGSLIIR, in which the sequences in the right stem were substituted by those from the left stem, also altering the SL-II structure. **(B)** Comparison of the cleavage efficiency between DVG12.7 and its compensatory mutants

(Fig. 1D) [14]. To determine whether the sequence or structure of stem–loop II where the cleavage site is located is also a factor affecting the cleavage efficiency, compensatory mutation was performed (Fig. 3A). As shown in Fig. 3B, when the structures of SL II were altered (DVGSLIIR and DVGSLIIL) or when the structures were maintained but the sequences were altered (DVGSLIIRL), the cleavage efficiency was decreased, suggesting that both

the sequence and the structure can affect the cleavage efficiency of DVG12.7.

The correlation of DVG12.7 cleavage with the characteristics of RNase L The results shown in Fig. 1C and D revealed that the preferred cleavage sites in DVG12.7 occur after UU and UA dinucleotides, which are located in the single-strand region of stem–loop II. Additionally, the factor leading to this cleavage is from cells instead of coronavirus. The aforementioned features fit the general criteria for RNA cleavage by cellular RNase L, among the known cellular RNases. Therefore, it is speculated that the cleavage features may be correlated with the characteristics of the cellular endoribonuclease RNase L. RNase L is a latent enzyme that is constitutively expressed in nearly every mammalian cell [31]. The RNase L monomer is inactivated; thus, the expression levels of RNase L may not represent its function in RNA cleavage [32]. Because (i) 2'-5'-oligoadenylate synthetase (OAS) can use ATP to synthesize 2',5'-linked oligoadenylates (2–5 A) and (ii) the synthesized 2–5 A is the sole factor which can cause inactive RNase L monomers to form activated RNase L dimers, leading to the cleavage of RNA, including rRNA, the level of OAS gene expression is an indicator of the level of activated RNase L, and rRNA cleavage provides functional evidence of the activation of RNase L [33–36]. Consequently, to examine the correlation of DVG12.7 cleavage with RNase L, DVG12.7 was transfected into HRT-18 cells and A549 cells. At 0.1, 1.5 and 3 hpt, total cellular RNA was collected and subjected to (i) electrophoresis on a formaldehyde–agarose gel to detect the cleavage of rRNA, (ii) RT–qPCR to quantify the levels of OAS mRNA and (iii) a Northern blot assay to detect the synthesis of clvDVG. In DVG12.7-transfected HRT-18 cells, (i) no rRNA cleavage was observed (Fig. 4A, left panel), (ii) basal levels of OAS mRNA were detected (Figures S1A and S1C), and (iii) the levels of OAS mRNA did not increase with time (Fig. 4A, right panel and Figure S1A). However, in A549 cells, (i) rRNA cleavage began at 1.5 hpt and became evident at 3 hpt (Fig. 4B, left panel), (ii) basal levels of OAS mRNA were detected (Figures S1B and S1C), and (iii) the levels of OAS mRNA increased with time (Fig. 4B, right panel and Figure S1B). On the other hand, in HRT-18 cells, the Northern blot assay revealed that DVG12.7 was cleaved, but the ratio of cleaved to uncleaved DVG12.7 was almost unchanged (Fig. 4C). In contrast, in A549 cells, the assay results suggested that both the amount of cleaved DVG12.7 and the ratio of cleaved to uncleaved DVG12.7 increased with time (Fig. 4D). In addition, the cleavage pattern of DVG12.7 was very similar to that of the hepatitis C virus genome cleaved by RNase L [18, 35].

In A549 cells, because the levels of OAS mRNA (Fig. 4B, right panel), cleaved rRNA (Fig. 4B, left panel) and cleaved DVG12.7 (Fig. 4D) increased with time, the cleavage of DVG12.7 in A549 cells was potentially correlated with the activation of RNase L. On the basis of these results (Figs. 4B and D), the cleavage of DVG12.7 in HRT-18 cells was assessed as follows. Because (i) it has been suggested that cells contain basal levels of OAS which can activate RNase L independent of IFN [37, 38], (ii) HRT-18 cells also contained basal levels of OAS mRNA (Figures S1A and S1C) and (iii) the levels of OAS mRNA (Fig. 4A, right panel) and cleaved DVG12.7 (Fig. 4C) did not increase with time and rRNA was not cleaved (Fig. 4A, left panel), it is speculated that, after transfection, DVG12.7 can be cleaved by RNase L, which is activated by the basal levels of OAS. However, because the levels of OAS and thus activated RNase L did not increase with time, the basal levels of activated RNase L are not sufficient to cleave rRNA. Consequently, this finding may explain why DVG12.7 can be cleaved immediately after transfection and why the ratio of cleaved to uncleaved DVG12.7 is almost unchanged (Figs. 2 and 4C) in HRT-18 cells. Given these results, the increased gene expression of OAS and the subsequent activation of RNase L in A549 cells are speculated to occur through the IFN signaling pathway via the 5'-triphosphate group and double-stranded RNA formed by DVG12.7, as evidenced by the increase in rRNA cleavage over time (Fig. 4B, left panel), leading to increased levels of DVG12.7 cleavage (Fig. 4D). Because (i) the cleavage pattern of DVG12.7 in A549 cells was correlated with activated RNase L levels and (ii) the cleavage patterns of DVG12.7 in HRT-18 cells and A549 cells are similar, although the level of cleaved DVG12.7 increases with time in A549 cells, the results suggest that the cleavage of DVG12.7 in HRT-18 cells may be correlated with a cellular endoribonuclease with the characteristics of RNase L.

Discussion

In the current study, it is suggested that the cleavage sites of DVG12.7 occur preferentially at the 3'-end of UU and UA dinucleotides located in single-stranded RNA (Fig. 1C and D). In addition, the context of genome structures where the dinucleotides UA and UU reside may affect the efficiency of DVG12.7 cleavage (Fig. 3). Furthermore, based on the results shown in Fig. 4B and D, the increased amounts of DVG12.7 cleavage with time are very likely due to the increased amounts of RNase L, as indicated by the increased levels of OAS mRNA and cleavage of rRNA in A549 cells. Based on the known cellular endoribonucleases, these features all indicate that the cleavage of DVG12.7 is correlated to the cellular endoribonuclease with characteristics of RNase L [16, 18, 23, 24], although other unidentified cellular endoribonucleases cannot be precluded.

As shown in Figs. 2 and 4C, in HRT-18 cells, the amounts of cleaved DVG12.7 were not increased with

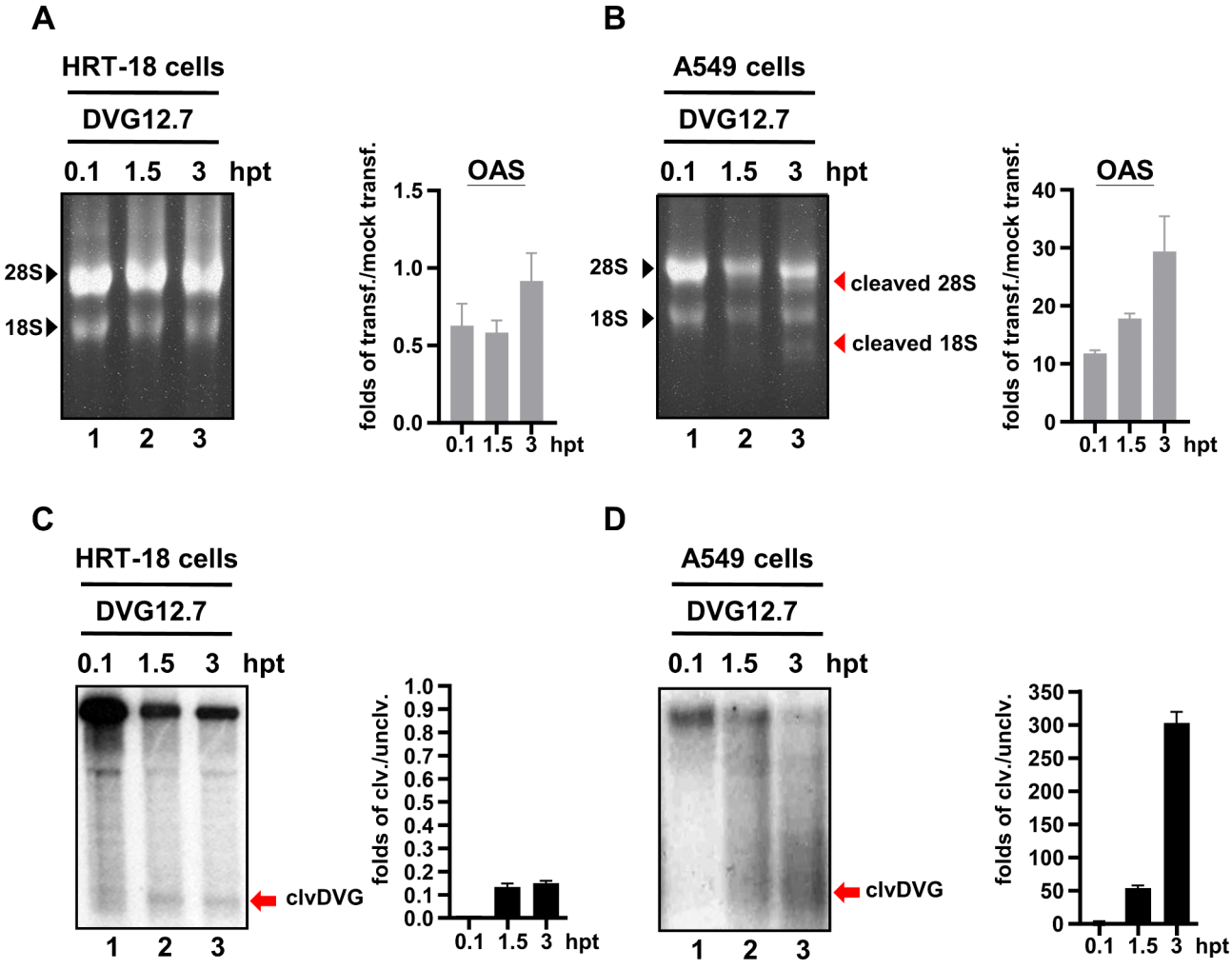

Fig. 4 Correlation of DVG12.7 cleavage with RNase L activity. **(A)** and **(B)** Left panels: HRT-18 cells **(A)** and A549 cells **(B)** were transfected with DVG12.7. At the indicated times, RNA was extracted and analyzed via a formaldehyde–agarose denaturing gel. The 18 S and 28 S rRNA bands are indicated by black arrows. The cleaved 18 S and 28 S rRNA products are indicated by red arrows. Right panel: The folds of OAS mRNA expression in transfected cells compared with mock-transfected cells (transf./mock-transf.) at different times (0.1, 1.5 and 3 hpt). "Mock" on the y-axis indicates the amount of mRNA detected from mock-transfected cells. The folds transf./mock-transf. on the y-axis are presented as relative units of mRNA compared with the amount of mRNA in mock-transfected cells (mRNA in mock-transfected cells = 1). **(C)** and **(D)** Left panels: HRT-18 cells **(C)** and A549 cells **(D)** were transfected with DVG12.7. At the indicated times, RNA was extracted and analyzed via Northern blotting. Right panel: Folds of cleaved DVG12.7 (clvDVG) over uncleaved DVG12.7 (unclv.)

time, and the ratio of cleaved vs. uncleaved DVG12.7 was almost unchanged. Because RNase L can be activated by the basal level of OAS independent of IFN induction [37], it is speculated that after the transfection of DVG12.7 in HRT-18 cells, the level of RNase L activated by the basal levels of OAS gene expression (Figure S1A and S1C) is sufficient to cleave DVG12.7 (Figs. 2 and 4C). However, because no IFN production was induced, as evidenced by the lack of rRNA cleavage over time (Fig. 4C), the levels of OAS gene expression (Fig. 4A, right panel) and thus those of activated RNase L did not increase with time. Consequently, once DVG12.7 is cleaved by basal levels of RNase L, no more DVG12.7 is cleaved, and the degradation of both uncleaved DVG12.7 and cleaved DVG12.7 (clvDVG) by other cellular RNases occurs over time, leading to a constant ratio between uncleaved DVG12.7 and clvDVG, as shown in Figs. 2 and 4C. This finding is supported by previous results showing that RNase L can be activated by basal OAS gene expression during early-stage infection independent of IFN induction [37]. The activation of basal-level RNase L by OAS, therefore, is also an antiviral mechanism that rapidly limits the spread of viruses. On the other hand, in A549 cells, in addition to the basal level of OAS gene expression (Figure S1B and S1C) [39], the levels of OAS gene expression (Fig. 4B, right panel) and the subsequent levels of activated RNase L are likely increased over time via IFN induction, as evidenced by the increased levels of rRNA cleavage (Fig. 4B, left panel). Consequently, the amounts of OAS gene expression and activated RNase L increase with time,

as do the amounts of clvDVG and the ratio between uncleaved DVG12.7 and cleaved clvDVG (Fig. 4D). Notably, while the results derived from A549 cells suggest that the cleavage of DVG12.7 in HRT-18 cells is caused by RNase L, we still have no direct evidence for this conclusion according to the current results. Thus, it is concluded that the cleavage of DVG12.7 in HRT-18 cells is correlated with a cellular endoribonuclease that has the characteristics of RNase L.

The results of this study unexpectedly identified suitable genome structures in coronavirus DVG that can be efficiently cleaved by cellular endoribonuclease with characteristics of RNase L. It is believed that the unidentified cellular endoribonuclease may also cleave the coronavirus single-stranded genome at the 3'-end of UA and UU dinucleotides in infected cells. However, because complicated secondary or tertiary structures can be formed on the genome in infected cells and RNA structures can also affect the cleavage efficiency of RNase L, as shown in this study, the unidentified cellular endoribonuclease may display different cleavage efficiencies at different locations of viral single-stranded RNA. This argument is supported by a study on hepatitis C virus in which the context of the genome can affect the RNase L cleavage efficiency [18].

In this study, we investigated the possible mechanism for the synthesis of an RNA fragment derived from coronavirus DVG. Our experiments suggested that the RNA fragment was a cleaved fragment of DVG12.7. Based on the findings that (i) the cleavage sites occurred predominantly after single-stranded UA and UU dinucleotides, (ii) the genome structures surrounding UA or UU dinucleotides affected the cleavage efficiency, and (iii) both the cleavage of rRNA and DVG12.7 were identified in A549 cells, we concluded that the cleavage of DVG12.7 is correlated with the cellular endoribonuclease with characteristics of RNase L. Such cleavage features have not been previously characterized in coronaviruses. Consequently, the current findings answer the question of how the shorter RNA fragments clvDVG is synthesized and further support the conclusions derived from the previous study [14].

Abbreviations

BCoV	Bovine coronavirus
UTR	Untranslated region
ORF	Open reading frame
TRS	Transcription-regulating sequence
DVG12.7	Defective viral genome 12.7
sgmRNA	subgenomic mRNA
HRT	Human rectal tumor
RACE	Rapid amplification of cDNA ends
clvDVG	Cleaved DVG.
A549 cells	Adenocarcinomic human alveolar basal epithelial cells
Tri	Transcript

Supplementary Information

The online version contains supplementary material available at https://doi.org/10.1186/s12985-024-02549-x.

Supplementary Material 1

Acknowledgements
We thank Dr. David A. Brian at University of Tennessee, Knoxville, for providing HRT-18 cells and BCoV. We thank Ruey-Yi Chang at National Dong Hwa University, Taiwan, for A549 cells.

Author contributions
Conceptualization: CHL and HYW; Methodology: CHL, HYL, FCH, CCY, CYY, HWH and HYW; Investigation: CHL, HYL and HYW; Resources: HYW; Writing—Original Draft: CHL and HYW; Writing—Review and Editing: CHL and HYW; Supervision: HYW; Funding Acquisition: HYW.

Funding
This work was supported by grant 113-2313-B-005-009-MY3 from National Science and Technology Council, Taiwan.

Data availability
No datasets were generated or analysed during the current study.

Declarations

Ethics approval and consent to participate
Not applicable.

Consent for publication
Not applicable.

Competing interests
The authors declare no competing interests.

Received: 16 August 2024 / Accepted: 18 October 2024
Published online: 01 November 2024

References

1. Brian DA, Baric RS. Coronavirus genome structure and replication. Curr Top Microbiol Immunol. 2005;287:1–30.
2. Gorbalenya AE, Enjuanes L, Ziebuhr J, Snijder EJ. Nidovirales: evolving the largest RNA virus genome. Virus Res. 2006;117(1):17–37.
3. V'kovski P, Kratzel A, Steiner S, Stalder H, Thiel V. Coronavirus biology and replication: implications for SARS-CoV-2. Nat Rev Microbiol. 2021;19(3):155–70.
4. Pasternak AO, Spaan WJ, Snijder EJ. Nidovirus transcription: how to make sense…. J Gen Virol. 2006;87(Pt 6):1403–21.
5. Wu HY, Brian DA. 5'-proximal hot spot for an inducible positive-to-negative-strand template switch by coronavirus RNA-dependent RNA polymerase. J Virol. 2007;81(7):3206–15.
6. Wu HY, Ozdarendeli A, Brian DA. Bovine coronavirus 5'-proximal genomic acceptor hotspot for discontinuous transcription is 65 nucleotides wide. J Virol. 2006;80(5):2183–93.
7. Brian DA, Spaan WJM. Recombination and coronavirus defective interfering RNAs. Semin Virol. 1997;8(2):101–11.
8. Lin CH, Chen B, Chao DY, Hsieh FC, Yang CC, Hsu HW, et al. Unveiling the biology of defective viral genomes in vitro and in vivo: implications for gene expression and pathogenesis of coronavirus. Virol J. 2023;20(1):225.
9. Zhou TRY, Gilliam NJ, Li SZ, Spandau S, Osborn RM, Connor S et al. Generation and Functional Analysis of defective viral genomes during SARS-CoV-2 infection. Mbio. 2023;14(3).
10. Lo CY, Tsai TL, Lin CN, Lin CH, Wu HY. Interaction of coronavirus nucleocapsid protein with the 5'- and 3'-ends of the coronavirus genome is involved in genome circularization and negative-strand RNA synthesis. FEBS J. 2019;286(16):3222–39.

11. Tsai TL, Lin CH, Lin CN, Lo CY, Wu HY. Interplay between the poly(A) tail, poly(A)-Binding protein, and Coronavirus Nucleocapsid protein regulates Gene expression of Coronavirus and the host cell. J Virol. 2018;92(23).
12. Wu HY, Guan BJ, Su YP, Fan YH, Brian DA. Reselection of a genomic upstream open reading frame in mouse hepatitis coronavirus 5'-untranslated-region mutants. J Virol. 2014;88(2):846–58.
13. Krishnan R, Chang RY, Brian DA. Tandem placement of a coronavirus promoter results in enhanced mRNA synthesis from the downstream-most initiation site. Virology. 1996;218(2):400–5.
14. Ozdarendeli A, Ku S, Rochat S, Williams GD, Senanayake SD, Brian DA. Downstream sequences influence the choice between a naturally occurring noncanonical and closely positioned upstream canonical heptameric fusion motif during bovine coronavirus subgenomic mRNA synthesis. J Virol. 2001;75(16):7362–74.
15. Garcia-Sastre A, Biron CA. Type 1 interferons and the virus-host relationship: a lesson in detente. Science. 2006;312(5775):879–82.
16. Silverman RH. Viral encounters with 2',5'-oligoadenylate synthetase and RNase L during the interferon antiviral response. J Virol. 2007;81(23):12720–9.
17. Li YZ, Weiss SR. Antagonism of RNase L is required for murine coronavirus replication in Kupffer Cells and liver sinusoidal endothelial cells but not in Hepatocytes. J Virol. 2016;90(21):9826–32.
18. Washenberger CL, Han JQ, Kechris KJ, Jha BK, Silverman RH, Barton DJ. Hepatitis C virus RNA: Dinucleotide frequencies and cleavage by RNase L. Virus Res. 2007;130(1–2):85–95.
19. Dong BH, Silverman RH. Alternative function of a protein kinase homology domain in 2',5'-oligoadenylate dependent RNase L. Nucleic Acids Res. 1999;27(2):439–45.
20. Zhou AM, Paranjape J, Brown TL, Nie HQ, Naik S, Dong BH, et al. Interferon action and apoptosis are defective in mice devoid of 2',5'-oligoadenylate-dependent RNase L. EMBO J. 1997;16(21):6355–63.
21. Dong BH, Xu LL, Zhou AM, Hassel BA, Lee X, Torrence PF, et al. Intrinsic molecular activities of the Interferon-Induced 2-5a-Dependent rnase. J Biol Chem. 1994;269(19):14153–8.
22. Cooper DA, Jha BK, Silverman RH, Hesselberth JR, Barton DJ. Ribonuclease L and metal-ion-independent endoribonuclease cleavage sites in host and viral RNAs. Nucleic Acids Res. 2014;42(8):5202–16.
23. Han JQ, Wroblewski G, Xu Z, Silverman RH, Barton DJ. Sensitivity of hepatitis C virus RNA to the antiviral enzyme ribonuclease L is determined by a subset of efficient cleavage sites. J Interf Cytok Res. 2004;24(11):664–76.
24. Silverman RH. Viral encounters with RNase L during antiviral innate immunity. J Interf Cytok Res. 2007;27(8):709–10.
25. Cooper DA, Banerjee S, Chakrabarti A, Garcia-Sastre A, Hesselberth JR, Silverman RH, et al. RNase L targets distinct sites in Influenza A Virus RNAs. J Virol. 2015;89(5):2764–76.
26. Tompkins WA, Watrach AM, Schmale JD, Schultz RM, Harris JA. Cultural and antigenic properties of newly established cell strains derived from adenocarcinomas of the human colon and rectum. J Natl Cancer Inst. 1974;52(4):1101–10.
27. Liao WY, Ke TY, Wu HY. The 3'-terminal 55 nucleotides of bovine coronavirus defective interfering RNA harbor cis-acting elements required for both negative- and positive-strand RNA synthesis. PLoS ONE. 2014;9(5):e98422.
28. Lin CH, Yang CY, Wang ML, Ou SC, Lo CY, Tsai TL et al. Effects of Coronavirus Persistence on the genome structure and subsequent gene expression, pathogenicity and adaptation capability. Cells-Basel. 2020;9(10).
29. Knoops K, Kikkert M, Worm SH, Zevenhoven-Dobbe JC, van der Meer Y, Koster AJ, et al. SARS-coronavirus replication is supported by a reticulovesicular network of modified endoplasmic reticulum. PLoS Biol. 2008;6(9):e226.
30. Paul D, Bartenschlager R. Architecture and biogenesis of plus-strand RNA virus replication factories. World J Virol. 2013;2(2):32–48.
31. Bisbal C, Silverman RH. Diverse functions of RNase L and implications in pathology. Biochimie. 2007;89(6–7):789–98.
32. Dong B, Silverman RH. 2-5A-dependent RNase molecules dimerize during activation by 2-5A. J Biol Chem. 1995;270(8):4133–7.
33. Schwartz SL, Conn GL. RNA regulation of the antiviral protein 2'-5'-oligoadenylate synthetase. Wiley Interdiscip Rev RNA. 2019;10(4):e1534.
34. Silverman RH, Skehel JJ, James TC, Wreschner DH, Kerr IM. Ribosomal-rna cleavage as an index of ppp(A2'p)na activity in Interferon-treated Encephalomyocarditis Virus-infected cells. J Virol. 1983;46(3):1051–5.
35. Han JQ, Barton DJ. Activation and evasion of the antiviral 2'-5' oligoadenylate synthetase/ribonuclease L pathway by hepatitis C virus mRNA. RNA. 2002;8(4):512–25.
36. Schroeder A, Mueller O, Stocker S, Salowsky R, Leiber M, Gassmann M et al. The RIN: an RNA integrity number for assigning integrity values to RNA measurements. Bmc Mol Biol. 2006;7.
37. Birdwell LD, Zalinger ZB, Li YZ, Wright PW, Elliott R, Rose KM, et al. Activation of RNase L by murine coronavirus in myeloid cells is dependent on basal Oas Gene expression and Independent of Virus-Induced Interferon. J Virol. 2016;90(6):3160–72.
38. Stark GR, Dower WJ, Schimke RT, Brown RE, Kerr IM. 2-5A synthetase: assay, distribution and variation with growth or hormone status. Nature. 1979;278(5703):471–3.
39. Banerjee S, Gusho E, Gaughan C, Dong BH, Gu XR, Holvey-Bates E, et al. OAS-RNase L innate immune pathway mediates the cytotoxicity of a DNA-demethylating drug. P Natl Acad Sci USA. 2019;116(11):5071–6.

Publisher's note